Experimental study on stability and rheological properties of aqueous foam in the presence of reservoir natural solid particles

Roozbeh Rafati *, Amin Sharifi Haddad, Hossein Hamidi
School of Engineering, Kings College, University of Aberdeen, AB24 3UE

Abstract:

Gas injection and especially CO_2 flooding has been applied in many oil reservoirs globally to increase oil recovery factor in addition to its environmental friendly aspects. However, difference between fluid viscosities and densities, can cause interface instability where gas override and fingering may expedite gas breakthrough. Different types of foam have been proposed to improve interface stability. Yet, a major uncertainty is interaction of foam with natural reservoir particles which may improve or downgrade the performance and stability of foam. In this study we examined foam stability through solid-fluids interactions between solid particles of hydrocarbon reservoirs and aqueous foam. We tested five common reservoir particles of calcium carbonate, calcium sulfate, barium sulfate, strontium sulfate and iron oxide with different surfactant and particle concentrations. It is found that stability of foam in the presence solid particles is a function of density, shape, size, and wettability of particles where monolayer, bilayer of network or particles stabilise foam lamella or rupture foam structure. Results show that solid particles of calcium carbonate, barium sulfate and strontium sulfate enhance the thermodynamic stability of foam. This is due to the distribution of semi-hydrophilic solid particles, which form mono- and multi-layers of particle chains in foam lamellae and plateau borders. On the other hand, solid particles of iron oxide and calcium sulfate destabilise foam where particle swelling, adsorbed surfactant solution and settlement into liquid phase due to their high densities were observed. The results suggest that a comprehensive study of liquid and solid interaction is critical in design of any foam for enhanced oil recovery processes.

*Corresponding author: Email: roozbeh.rafati@abdn.ac.uk, Tel: +44 1224 272497

Keywords:

Foam Stability, Foam Apparent Viscosity, Solid Particles, Enhanced Oil Recovery, Solid-Fluids Interactions, Gas Mobility Control

Introduction

Gas injection and CO_2 flooding as enhanced oil recovery methods have been used successfully in many places around the world. In this kind of processes injected gas phase displaces oil through reducing interfacial tension and capillary effects, which improves ultimate recovery factor. However, high gas to oil mobility ratio is an unfortunate that causes gravity override, gas phase channelling, and viscous fingering. Therefore, high gas to oil mobility ratio results in poor sweep efficiencies and early breakthrough of displacing phase (gas) [1-3].

In gas injection processes, stability of displacing front is a main concern, and it is a function of many variables such as injection pressure, oil viscosity, type of the injected gas, miscibility conditions, among others. Previous studies were conducted to improve the stability of displacing front in gas injection processes such as miscible gas injection, water alternating gas injection and foam flood [4-12]. Miscible gas injection is designed to mobilize oil as a single phase flow in porous media and avoid two phase flow system and capillary effects, therefore gas may not breakthrough as a second phase [1-3, 11-13]. Similarly, in water alternating gas injection, a slug of injected gas is followed by a slug of water to decrease the likelihood of early gas breakthrough while decreasing capillary effect through gas phase in porous media.

While there are many successful projects based on these recovery methods, difficulty in control of processes, cost of high pressure gas injection for miscible gas flood, and oil trapping by water phase in water alternating gas process, are challenges in place [11-14].

Another solution to control gas mobility and increase gas front stability is the use of surfactant-stabilised foam. This idea was first introduced by Bond and Holbrook in 1958[15], and later many other investigations have been conducted on characterisation and use of foam in gas injection process [16-22].

Foam improves the performance of gas flooding processes through two mechanisms: first, the presence of a foaming agent and aqueous phase creates more favourable mobility ratio of displacing to displaced fluids, and second, gas diversion from the fractures and high permeability zones to lower permeability regions can take place, where both of these mechanisms increase the stability of displacing front and reduce the early breakthrough of gas [17, 23-25].

Despite these favourable properties, foam is not thermodynamically stable and its physical structure can break down easily when two bubbles approach each other. This collapse in the structure of foam happens as liquid film between adjacent bubbles undergoes thinning, and as a result liquid film can rupture [25-27]. Various methods have been proposed to improve foam stability, such as increasing surfactant concentration, mixing different types of surfactants, and addition of co-surfactants and polymers to foaming agents. These solutions create a stable liquid film between bubbles which is called meta-stable super-thin film state, however, they are often expensive and might not be economical for large scale applications. Furthermore, these remedies may alter physical properties of the reservoir rocks that could result in a poor flow conductivity in porous media. Therefore, a thorough analysis of rock-fluids interactions is critical for the use of different compositions of foam in hydrocarbon reservoirs.

Foam stability can also be affected by the presence of dissolved species in other phases, such as second liquid phase containing fine solids. These species are naturally in the reservoir that may stabilise or destabilise the structure of foam. Foam stability in this condition is a factor

of different parameters; firstly whether the solid species are strongly liquid affinitive and there is a tendency to be accumulated at the gas-liquid interface or not, and secondly, what are the impacts of accumulated particles on the interfacial properties and lamellae viscosities of gas-liquid interface.

Concentration of solid particles in liquid phase, their wettability, size and shape are critical parameters affecting bulk foam stability [28-39]. Concentration of solid particles defines the quantity of particle association in foam lamellae and at the plateau borders, which is a key factor for apparent viscosity enhancement of bulk foam [38-42].

Foam stability of silica and laponite particles at various concentrations with mixture of anionic and non-ionic surfactants were studied by many researchers [30-34, 36, 38, 39, 43, 44]. A synergistic foam stability trend was reported, where it shows more prominent effects with increasing in the concentration of particles. The enhancement of synergistic effect is attributed to an increase in the density of adsorbed particle. At low-to-moderate surfactant concentrations, foam stability increases about 20% compared to the mixtures that have pure hydrophilic particles. The rationale for such improved stability is low surfactant concentrations where bridging flocculation of particles at foam interface produces enlarged and sterically strong interfacial barriers. Furthermore, at moderate surfactant concentrations, surface elasticity increases due to the presence of suspended particles in surfactant solution.

Horozov (2008) suggested the probable mechanisms which foam lamella stabilisation may take place. His suggested first mechanism is layering of solid particles inside liquid film and categorised them as a monolayer of bridging particles; a bilayer of close-packed particles and a network of particle aggregates (gel) [32]. Second, foam stabilising mechanism by particle comes into play if the particles are not completely water-wet. In this case particles tend to aggregate at foam-liquid interface where they may improve the mechanical stability of lamellae. On the other hand, strongly hydrophobic particles may behave differently, and

destabilise foam structure. It was reported that intermediate contact angles (between about 40° and 70°) would be optimum to develop a solid-stabilised foam [30, 32-34, 39, 41].

Analogous bridging mechanisms have been suggested for antifoaming behaviour of hydrophobic particles or mixtures of particles and oil [25]. Hydrophobic particles create a convex shape curvature on the surface of film at gas-liquid interface; thus capillary pressure decreases the thickness of liquid film. For hydrophilic particles, liquid film exhibits a concave meniscus at its surface; where capillary pressure is exerted in gas phase in opposite direction [45]. Furthermore, it should be noted that based on previous investigations, particles with rough edges on their surface, commonly found in commercial antifoams, can cause rapture in liquid film at even contact angles less than 90°. Consequently, rough hydrophobic particles are more effective antifoam agents than smooth particles, and therefore rounded solid particles stabilise bulk foam [45].

Alargova (2004) demonstrated that rod-shape particles can act as effective foam stabilisers in the presence of sodium dodecyl sulfate (SDS) surfactant [46]. They used rod-shape polymer particles with an average length of 23.5 μm and diameter less than 1 μm, which exhibited a contact angle of $\theta \approx 80°$ at the air-water surface through the surfactant solution. Their fairly dilute micro-rod suspensions (0.2–2.2 wt%) in pure water, produced foam upon shaking and it showed remarkably a stable structure which last for more than three weeks even under drying conditions in an open vessel [46].

Nowadays, silica and metal nanoparticles are frequently used as a foam stabiliser agent for enhanced oil recovery processes [38, 39, 41, 47]. It was found that nanoparticles at concentrations between 0.05 - 2 wt% can stabilise foam in the presence of both non-ionic and anionic surfactants. These types of nanoparticle foam are two to eighteen times more stable compared to the same foam without nanoparticles in its structure [34, 38, 39, 41, 47].

Properties and performance of particle-stabilised foam have been investigated by many researchers [30-33, 36-40, 42, 43, 47-50]. However, the effects of scales and precipitates, such as natural particles in porous media, on foam stability and foam flooding performance have not been investigated. In this study, we explored effects of such naturally occurring particles on the properties of foam. A series of experiments were performed to evaluate the effects of solid particles on foam stability, foam texture and foam apparent viscosity. It can improve our understanding of foam flooding process, its design and performance for any specific reservoir. In the other words, the key findings from this work have potential significance in foam flooding in reservoirs with inherent large quantities of scale and precipitates, including offshore foam injection in the presence of divalent and trivalent cations.

Experimental setup and procedure

In this study, three sets of experiments were performed. First set of experiments is related to bulk foam stability where we evaluated stability of bulk foam in the presence of different solid particles with different concentrations of surfactant. We measured foam height and its half life time in these experiments [51, 52]. Second set of experiments deals with foam texture analysis. In these experiments we used stereo microscope and image processing tools to identify the average bubble size in the presence of different solid particles [53]. And the last set of experiments is designed to find foam apparent viscosity in the presence of different particles with the use of capillary tube [54].Research strategy and details of each set of experiments are summarized in Table 1.

Table 1: Basic property measurements

Experiment Name	Purpose	Equipment/ Method
Bulk foam stability test	Evaluate bulk foam stability with respect to solid particles and surfactant concentration	Foam height measurement /half life
Foam texture analysis	Estimate bulk foam average bubble size in the presence of solid particles	Stereo microscope and image processing
Bulk foam apparent viscosity investigation	Investigate bulk foam apparent viscosity in the presence of solid particles	Capillary tube method

Sulfotex AOS (Alpha Olefin Sulfonate) was used as a surfactant, and was supplied by the Henkel Company with the quality of 60% active in the solution, viscosity of 1cp, and pH of 7.5. Alpha Olefin Sulfonate (AOS) has been widely used in enhanced oil recovery processes as it is effective in attaining low interfacial tension. Furthermore, it is relatively inexpensive and chemically stable surfactant, as it doesn't adsorb on the surface of the majority of reservoir rocks because of the negative charge on the head group of its molecule [3, 41]. Solid particles with 99% purity and different range of sizes were used (provided by Sigma Aldrich). List of solid particles and their properties are presented in Table 2.

Table2: List of reservoir occurring solid particles used in this study

Name	Chemical Formula	Density g/cm^3	Solubility in 100 mL Water (25°C)	Average Diameter μm
Calcium Carbonate	$CaCO_3$	2.71	0.15 g	12.16
Calcium Sulfate	$CaSO_4$	2.96	0.21 g	7.61
Barium Sulfate	$BaSO_4$	4.50	0.000285 g	1.38
Strontium Sulfate	$SrSO_4$	3.96	0.0135 g	64.14
Iron oxide	Fe_2O_3	5.24	0.0000011 g	131.04

Physical model used in this study, is shown in Figure 1. It consists of a transparent cylinder with the volume of 1000 mL, which is fixed with a clamp system in a bath. Bath was used to regulate the temperature of the graduated cylinder during each experiment. It provides

an isothermal condition with the accuracy of 1°F at the temperature of 75°F, and a maximum of 200°F. A crystalline alumina gas diffuser with diameter of 25.4 mm is located inside the cylinder. The gas diffuser has a maximum pore diameter of 80µm and was calibrated with the standard of ASTM D892-06. CO_2 supply provides gas flow rate of 94 mL per second through gas diffuser and cumulative volume of CO_2 passing through upper exit of cylinder was measured using a volumetric flask. It should be noted that all experiments were conducted in the absence of oil.

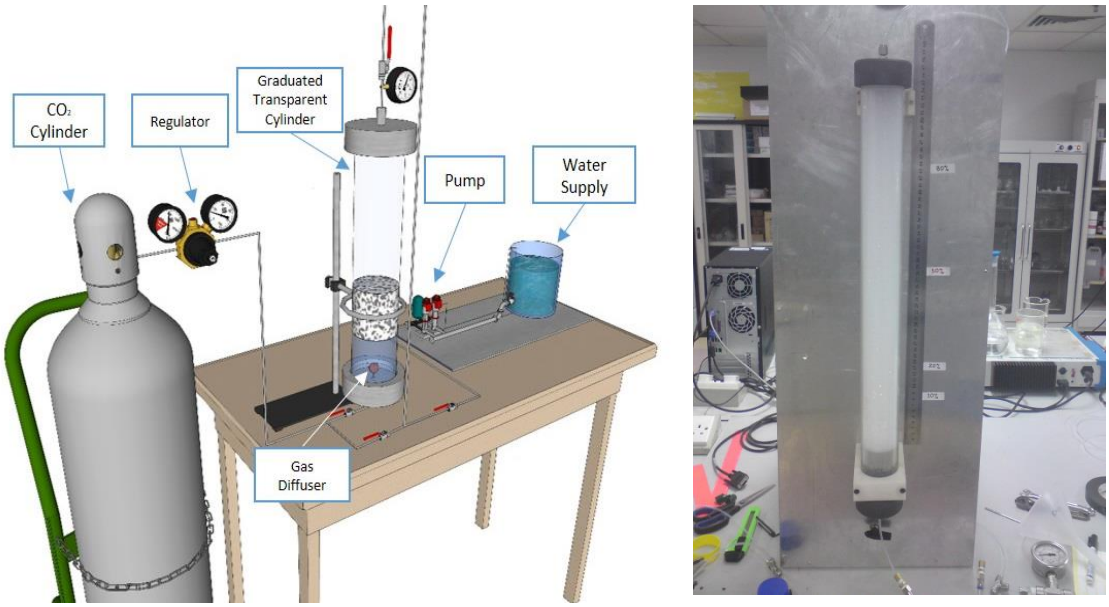

Figure 1. Schematic diagram of the apparatus used in foam generation

Surfactant solutions with different concentrations were mixed gently with de-ionized water. Then, surfactant solution was slowly poured into the transparent test cylinder. To perform an accurate bulk foam stability test, surfactant solution should completely cover porous gas diffusing stone. Flow pressure was set at 3.45 kPa. Foam was generated with flow of carbon dioxide into the cylinder for 25 seconds, before we start measuring the initial and final heights of foam. Foam drainage was recorded every 1 to 3 minutes following foam

generation process. Results are comparable with the presented trend of bulk stability tests patented by Klaus et al. 2004 (Figure 2) [51].

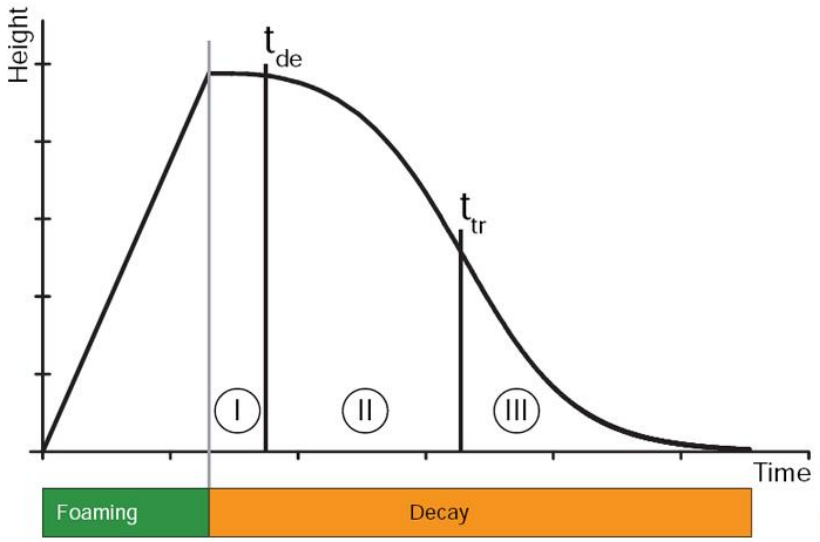

Figure 2: Standard foam stability plot [51]

Figure 2 indicates that foam lifetime might be divided into two sections, namely "foaming" and "decay" sections, which are shown with green and orange colour zones, respectively. Foaming section corresponds to foam generation and maximum height which is the difference between the top of foam and liquid solution that is maintained until the deviation time, t_{de}. Maximum height stays unchanged until deviation time, t_{de}, at which liquid films inside foam begin to rupture. A transition time, t_{tr}, corresponds to the half-life of foam with respect to its maximum height. Foam drainage beyond transition time can also be used to describe foam stability, i.e., $t_{tr} < 10$ seconds corresponds to unstable foam, whereas $t_{tr} > 10$ seconds corresponds to meta-stable foam; the longer transition time, the more stable foam system [51].

To evaluate bulk foam texture (average bubble size), images of bulk foam in the presence and absence of solid particles were captured. Figure 3a shows a 24 bit picture taken from the cross sectional area of the cylinder. It was analysed using IMAGEJ digital image processing

201 software. Analysis requires conversion of 24-bit image to 8-bit image where an edge
202 detection algorithm can be applied. Thresholding yields binary images (Figure 3b), which are
203 then calibrated using histogram equalization to minimise differences between the image
204 acquisition procedures (Figure 3c) and the average foam bubble size is extracted. In the next
205 step, similar tests were conducted in the presence of different solid particles to identify their
206 effects on bulk foam stability. Then, to characterise solid particle size and shape, high
207 resolution SEM images of particle samples after drying them for 24 hours in an oven at the
208 temperature of 100°C, were analysed using an image processing tool, IMAGETOOL [53].

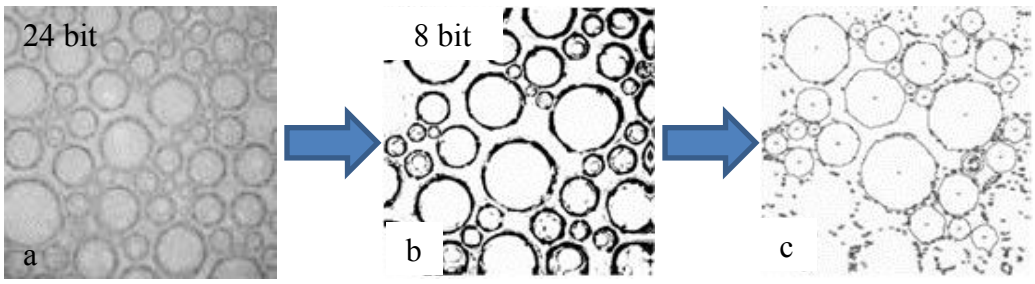

209

210 Figure 3: Bubble size determination using IMAGEJ software: (a) 24-bit coloured foam
211 image, (b) 8-bit image and (c) histogram equalisation and average bubble size determination

212

213 Apparent viscosity of bulk foam was determined by capillary tube method, using foam with
214 continuous foam quality of 80±5% with a flow rate of 4 mL per minute at 25°C. Apparent
215 viscosity of bulk foam was measured using a capillary tube with the length of 25 cm and
216 diameter of 2 mm, where flow rates were between 100-500 mL per hour. Then viscosity at
217 different shear rates can be measured.

218 Pressure difference across capillary tube with flow of surfactant solution was measured every
219 sixty seconds to achieve a stabilised differential pressure. The flow of initial pre-generated
220 foam was directed through the capillary assembly bypass in order to allow the flow rate and
221 texture of the generated foam to be stabilised. Upon attaining bubble uniformity, foam was

directed through the capillary tube assembly and the differential pressure across the tube was measured using data-acquisition system. Poiseuille's equation (Equation 1) was used for fluid flow through a horizontal tube with circular cross-sectional area, to calculate the apparent viscosity, μ_{app},:

$$\mu_{app} = \frac{\pi R^4 \Delta P}{2QL}\left[\frac{n}{3n+1}\right] \quad (1)$$

where R (cm) is the radius of capillary tube, ΔP (atm) is pressure drop across capillary tube, Q (cm^3/sec) is the flow rate of foam, L (cm) is the length of capillary tube and *n* is the power-law fluid index, which in this study, it was assumed to be 0.7 for foam quality in the range of 80-90% [54] .

Since it is assumed that foam is a non-Newtonian fluid, viscosity was determined with respect to the shear rate through Equation 2:

$$\dot{\gamma}_w = \frac{Q}{\pi r^3}\left[\frac{3n+1}{n}\right] \quad (2)$$

where $\dot{\gamma}_w$ is the shear rate (1/sec). Foam flow through smooth capillary tubes at flow rates of 100, 300, 500 and 1000 mL per hour and foam quality of 80% was conducted. Based on the monitored data, one can develop graph of apparent viscosity versus shear rate. This test has been conducted for foam flow in the presence of different solid particles. In the following section results of different tests and detailed analyses were presented.

Results and discussion

In the first series of experiments bulk foam was generated with Alpha Olefin Sulfonate (AOS) at different concentrations (50, 100, 200, 500, 1000 and 5000 ppm). Generated foam was used to understand the behaviour of bulk foam without the presence of other phases.

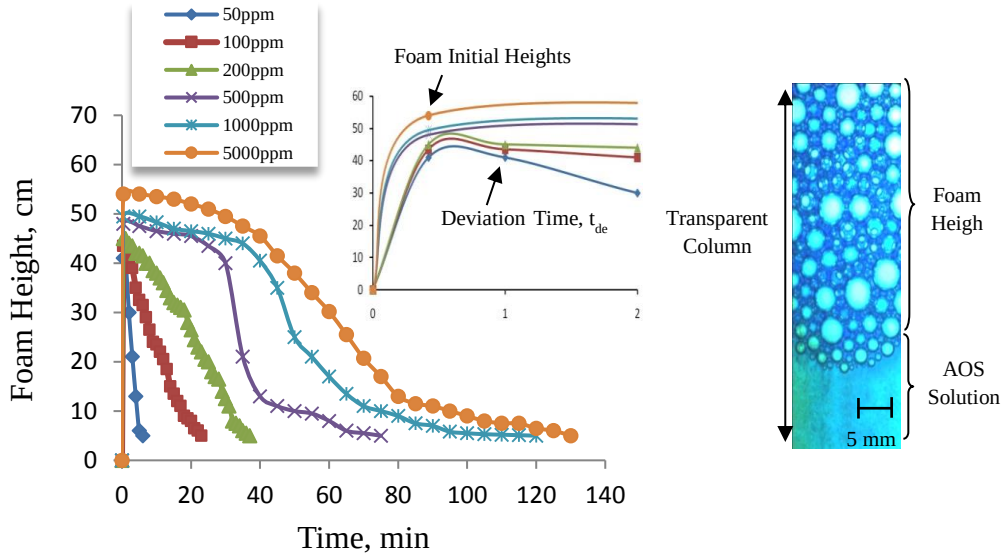

Figure 4: a) bulk foam stability for different concentrations of AOS, b) a sample image of foam stability test in a transparent cylinder (scale size of 5 mm is shown) [1 ppm of AOS solution = 3.17×10^{-6} mol/L]

Figure 4 shows the effect of surfactant concentration on foam height and its stability. It can be seen that higher surfactant concentration enhances bulk foam stability and also the maximum foam height. Inset plot of Figure 4 magnifies first two minutes of foam stability test. It shows that AOS bulk foam with concentrations less than 500 ppm exhibit different profiles in the first thirty seconds compared to foam with higher concentrations of surfactant (foam agent). This might be attributed to intermolecular forces; such as capillary, gravity, viscous and elasticity forces. These interactions are dominant in the lamellae and at the plateau borders which are critical for foam stability at lower concentrations. On the other hands at higher concentrations of surfactant, foam stability is predominantly developed by micelles formation. Due to these molecular interactions, foam that corresponds to higher concentrations of surfactant has more stable behaviour as shown in Figure 4, where concentrations more than 500 ppm show a plateau trend for a period of time, before the

collapse in foam structure. These results are consistent with the reported behaviour of foam stability by *Osei-Bonsu et al.*, 2011 [55]. They showed that foam that is generated using lower concentrations of AOS has a significant tendency to be ruptured, which leads to a rapid draining process; (e.g. 50 ppm AOS solution).

In the rest of this study we explored the effect of naturally occurring solid particles on foam generated with different concentrations of surfactant. In the first series of solid particle tests, we used calcium carbonate. The effects of calcium carbonate, 0.05-1 wt%, on bulk foam stability generated from 200, 500, 1000, and 5000 ppm AOS solutions were evaluated.

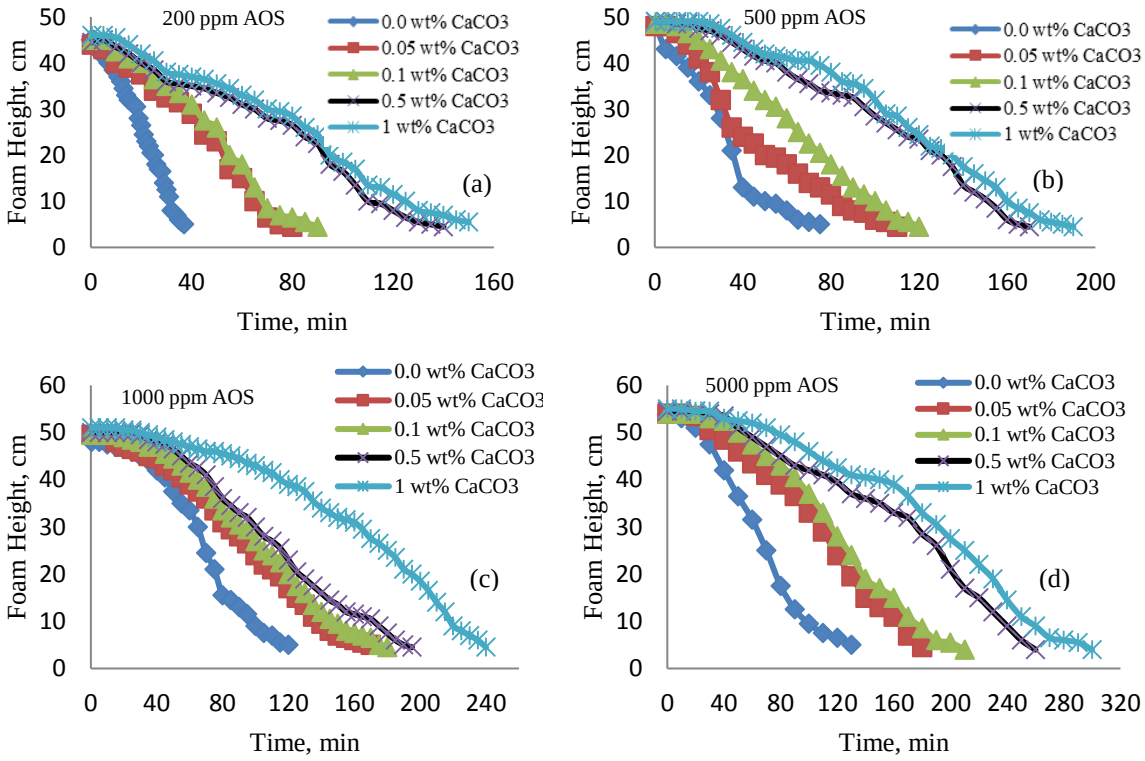

Figure 5 : bulk foam stability in the presence of calcium carbonate solid particles at different concentrations of AOS, (a) 200 ppm (b) 500 ppm , (c) 1000 ppm , (d) 5000 ppm [1 ppm of AOS solution = 3.17×10^{-6} mol/L]

Figure 5 shows improved bulk foam stability in the presence of calcium carbonate. There is no chemical reaction to be considered, however, it seems solid-fluids interactions of

suspended particles and foam result in an effect associated with apparent viscosity enhancement and average bubble size reduction.

Suspended particles attract bubbles, and liquid film of bubble sticks on the surface of particles where the chance of bubble coalescence decreases and as a result bubbles stay small and do not merge into each other, therefore foam structure breaks down at a longer time period. Also these interactions as a balance between capillary, gravity, viscous and elasticity forces, create a resistance to flow for foam, which in turns increases apparent viscosity of foam. This behaviour has been observed in the experiments where apparent viscosity of foam increased by about 0.2 cp in the presence of calcium carbonate at different shear rates as shown in Figures 6.

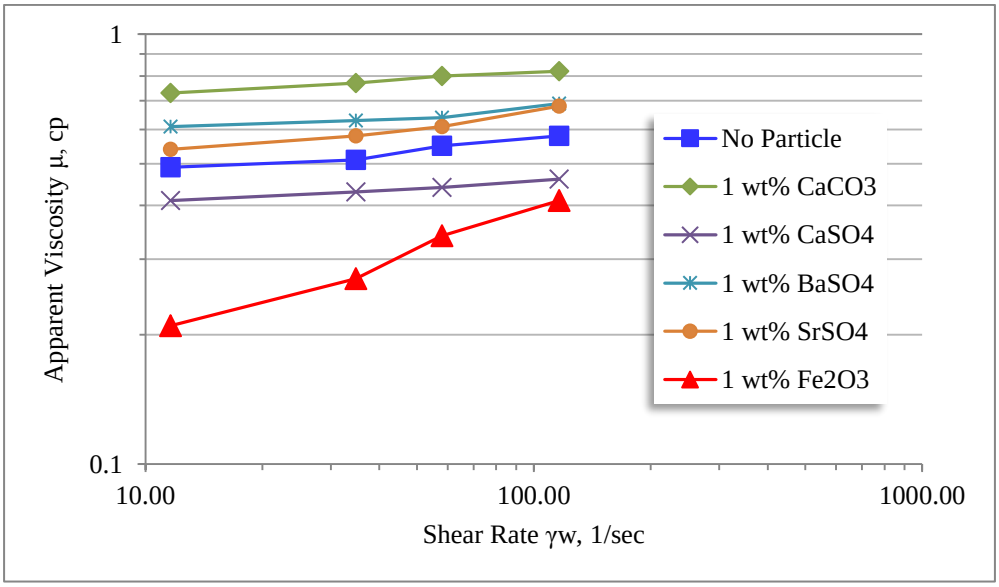

Figure 6: Comparison of bulk foam apparent viscosities versus shear rate in the absence and presence of 1 wt% of: calcium carbonate, calcium sulfate, barium sulfate, strontium sulfate and iron oxide.

Foam texture is also affected by the same solid-fluids interactions in the presence of such particles. As particles have a tendency to stay on the surface of foam bubbles, and consequently avoid bubble from merging into adjacent bubbles, the average bubble size

(diameter) reduces from about 6 mm (in the case of pure foam) to 2.75 mm (in the presence of suspended calcium carbonate), therefore, majority of bubble sizes were found to be in the range 1-4 mm (Figure 7). It is shown that bubble size distribution changes from right skewed shape (b) to left skewed shape (a), due to addition of solid calcium carbonate particles. These particles avoid the enlargement of bubbles and their film rupture. On the other side, bubbles in pure foam can easily merge into each other and create larger bubbles which are thermodynamically unstable and film rupture would happen fast.

And as a result, decrease in the average bubble size diameter translates into a more stable bubble structure, which can be achieved through a thicker lamellae and plateau borders.

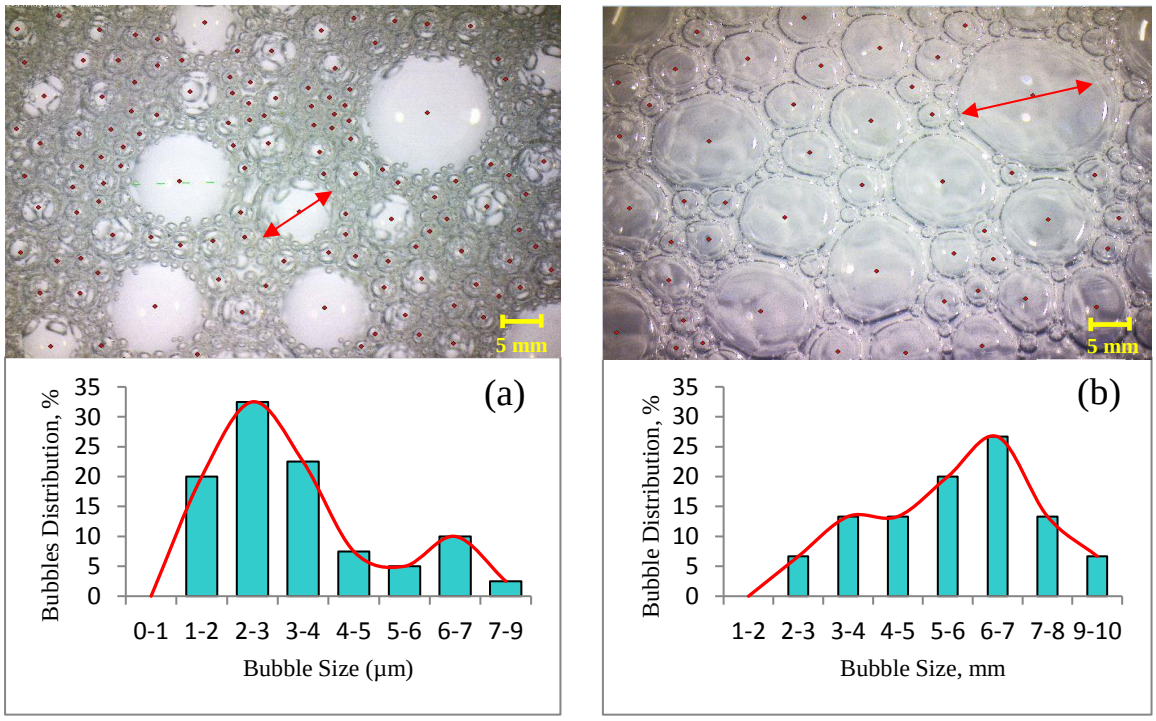

Figure 7: Bubble size distribution (a) in the presence of calcium carbonate particles, (b) in pure foam (in the absence of calcium carbonate particles)

Similar trend was observed at higher surfactant concentrations, as it is shown in Figure 5(d), prominent enhanced foam stability was developed. These results show that surfactant solution of 5000 ppm AOS in the presence of 1 wt% calcium carbonate is able to maintain foam

316 structure for approximately 300 minutes; more than twice the life span of foam in the absence
317 of calcium carbonate particles.
318
319 Next series of experiments were conducted for calcium sulfate particles (0.05-1 wt%). Unlike
320 calcium carbonate, calcium sulfate appears to destabilise foam generated by surfactant
321 solution of AOS, with concentrations between 200-5000 ppm as shown in Figure 8. This
322 might be due to high tendency of sulfate particles to adsorb water which makes the lamellae
323 and plateau borders thinner and eventually leads to bubble rupture. This destabilising effect is
324 supported by the results observed in apparent viscosity tests (Figure 6). Apparent viscosity
325 was decreased in the presence of calcium sulfate; by about 0.1 cp. Figure 8 shows the degree
326 of foam destabilisation for various AOS solutions at different particle concentrations. For
327 example for the solution of 1000 ppm of AOS, the duration of bulk foam collapse is
328 approximately 51 minutes in the presence of 1 wt% calcium sulfate, which is less than half of
329 the period that observed for foam in the absence of calcium sulfate (120 minutes). Based on
330 the results shown in Figure 8, it should be noted that destabilisation effects can be seen for all
331 solutions, however it is more dominant at lower surfactant concentrations. Therefore, foam
332 generated by lower surfactant concertation is more prone to instability source of calcium
333 sulfate particles. Foam destabilisation occurs when calcium sulfate particles adsorb surfactant
334 solution in foam lamella and plateau border which rapidly changes the aqueous foam from
335 wet to dry. Dry foam can break easily as the lamellas become very thin, and interfacial
336 tension in foam lamellas increases as the surfactant solution gets adsorbed on the surface of
337 the calcium sulfate.
338

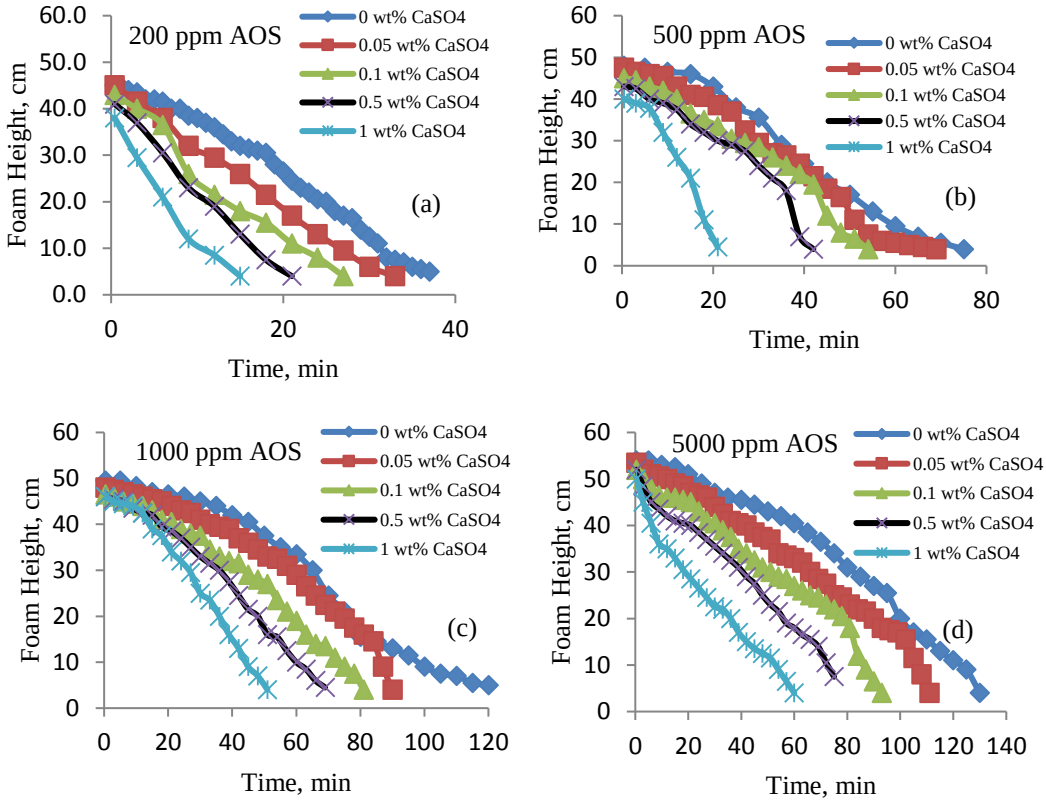

Figure 8 : Foam stability in the presence of calcium sulfate at different concentrations of AOS (a) 200 ppm, (b) 500 ppm, (c) 1000 ppm, (d) 5000 ppm [1 ppm of AOS solution = 3.17×10^{-6} mol/L]

Another type of solid particles that naturally exist in the reservoir is Barium Sulfate. We examined their effects on foam and results are presented in Figure 9. It indicates the addition of barium sulfate (0.05-1 wt%) to surfactant solution of AOS with concentrations between 200-5000 ppm, increases the stability of bulk foam compared to foam in the absence of solid particles. It can be seen from Figure 9 that foam stability in the presence of barium sulfate particles was slightly improved for all solid concentrations.

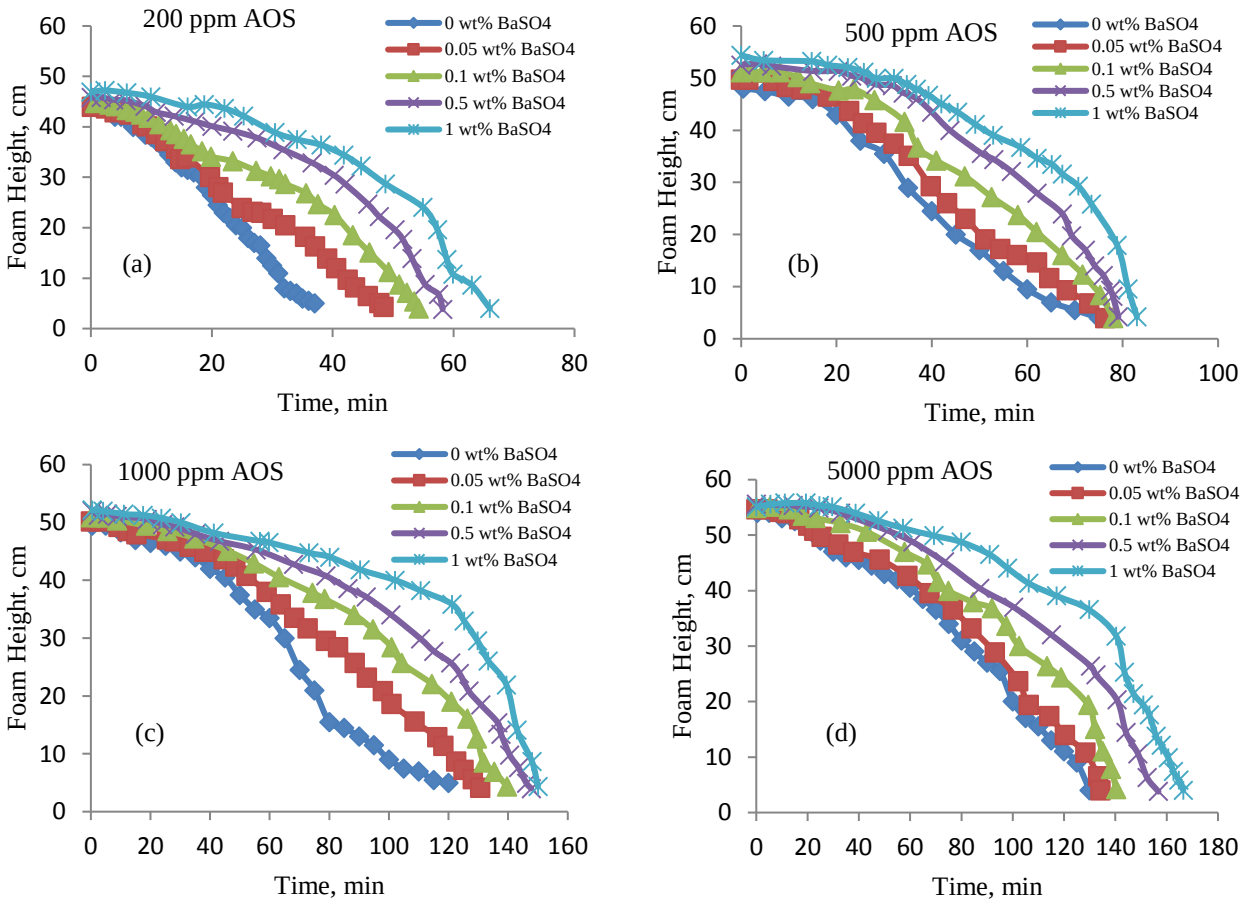

Figure 9 : Bulk foam stability in the presence of barium sulfate at different concentrations of AOS (a) 200 ppm, (b) 500 ppm, (c) 1000 ppm, (d) 5000 ppm [1 ppm of AOS solution = 3.17×10^{-6} mol/L]

The reason for foam stability enhancement is due to the physical properties of barium sulfate particles. These particles are very small (average diameter of 1 µm) and exhibit an intermediate degree of hydrophilicity, which results in a smaller and more homogeneous bubble size distribution. These small solid particles form multi-layered connected chains (particle gel) within foam structure. Developed chains increase the thickness of lamellae and plateau borders which result in a more viscous bulk foam as it was observed during apparent viscosity measurements (Figure 6). However, barium sulfate particles have relatively high density (4.4 g/mL), which means there is a larger gravity force, therefore, this decreases the

overall stability of foam compared to lighter solid particles. As a result barium sulfate multilayer slugs were separated from foam lamellae and plateau borders after some time, and they sink down into the surfactant solution, as shown in Figure 10.

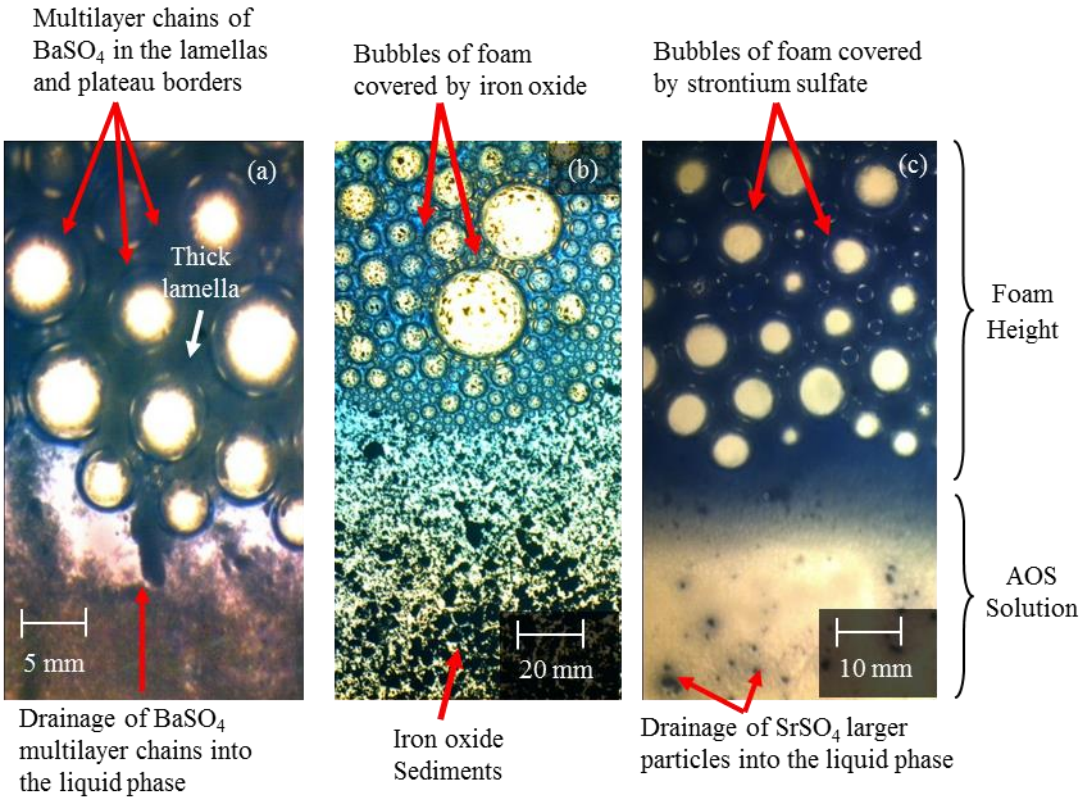

Figure 10: Foam stability and drainage of a) barium sulfate multilayer particles (particle gel), b) iron oxide and c) strontium sulfate

Forth type of solid particles used in this study was strontium sulfate particles. The results of the addition of strontium sulfate (0.05-1 wt%) to the surfactant solution of AOS with concentrations between 200-5000 ppm are presented in Figures 11. These results indicate that the presence of strontium sulfate increases bulk foam stability. Strontium sulfate particles with the density of 3.69 g/mL give this enhanced stability through increased viscosity in a similar manner to barium sulfate particles; however the size and shape of the larger strontium particles impinges on the degree of enhancement and can lead to drainage. Figure 11 shows

different surfactant solutions of AOS have more stability in foam structure in the presence of various strontium sulfate concentrations. As it can be seen, increased foam stability, manifested at higher surfactant concentrations.

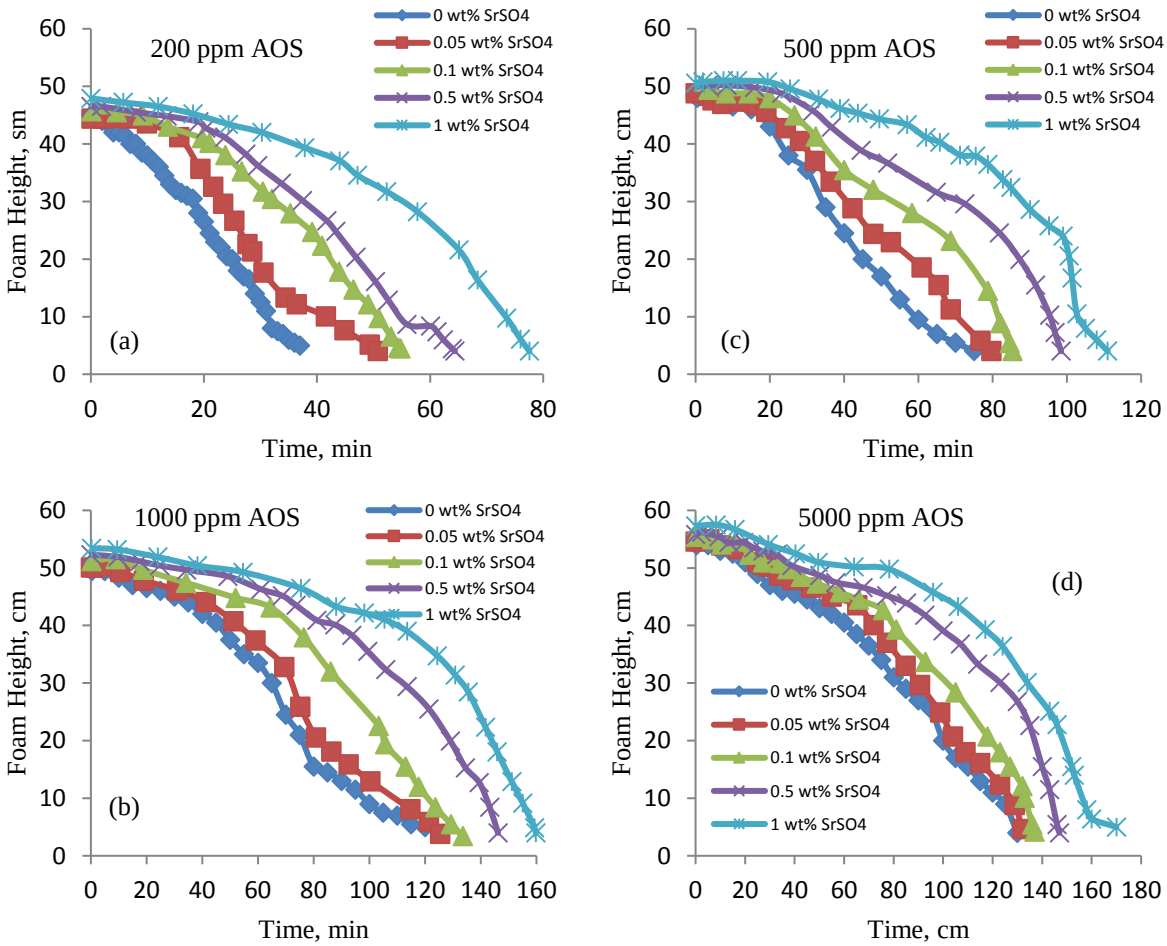

Figure 11: Foam stability in the presence of strontium sulfate at different concentrations of AOS (a) 200 ppm, (b) 500 ppm, (c) 1000 ppm, (d) 5000 ppm [1 ppm of AOS solution = 3.17×10^{-6} mol/L]

Last type of solids used in this study is iron oxide particles. Iron oxide particles are magnetic particles which have good capacity of heat transfer through foam structure. The results of foam stability test show that the addition of iron oxide (0.05-1 wt%) to surfactant solution of

AOS with concentrations between 200-5000 ppm, significantly destabilises foam. Iron oxide is denser than other particles, and significantly larger in size with hydrophilic properties which fall down through lamellas and lead to an increase of disjoining pressure and interfacial tension in the thin liquid films between gas bubbles. These characteristics of iron oxide cause rapid foam degradation even at high surfactant (AOS) concentrations. Figure 10b shows that larger black spots were deposited in surfactant solution which left foam structure due to gravity force and bubbles can merge into each other fast. Exhibited instability was confirmed with apparent viscosity measurements which indicated that iron oxide particles decrease bulk foam apparent viscosity (Figure 6).

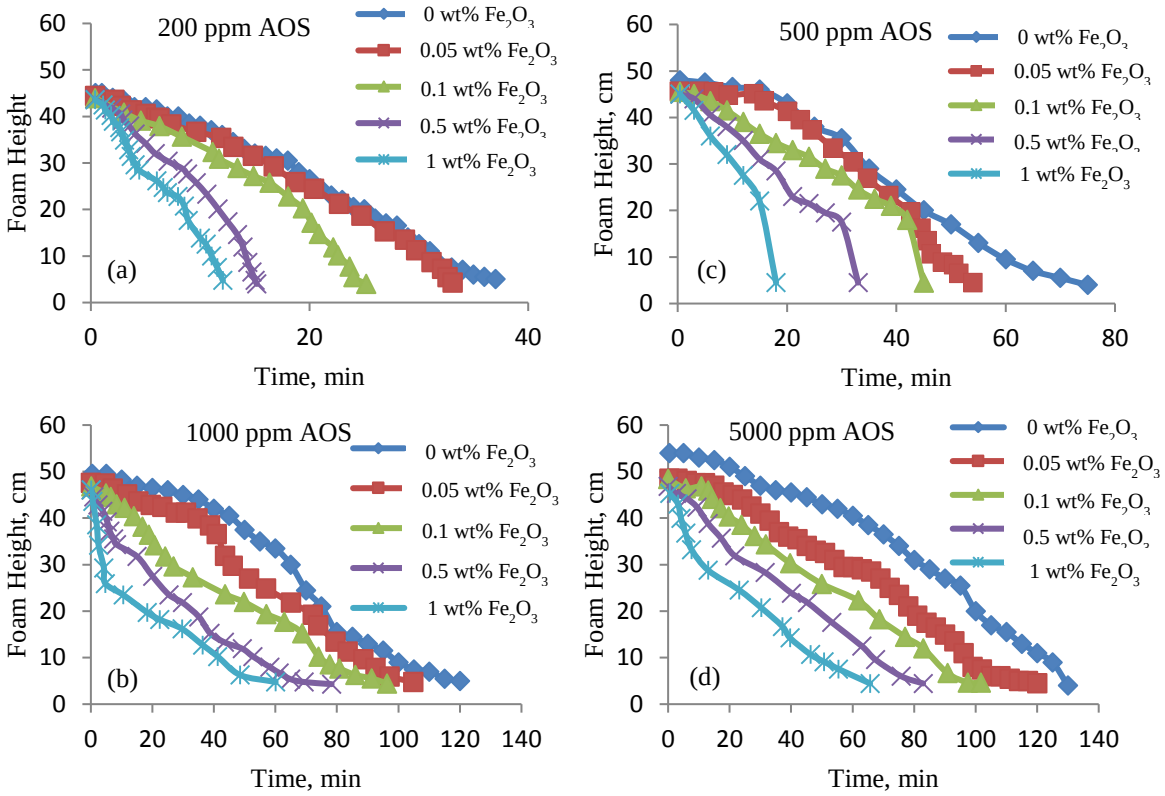

Figure 12: Foam stability in the presence of iron oxide at different concentrations of AOS (a) 200 ppm, (b) 500 ppm, (c) 1000 ppm, (d) 5000 ppm [1 ppm of AOS solution = 3.17×10^{-6} mol/L]

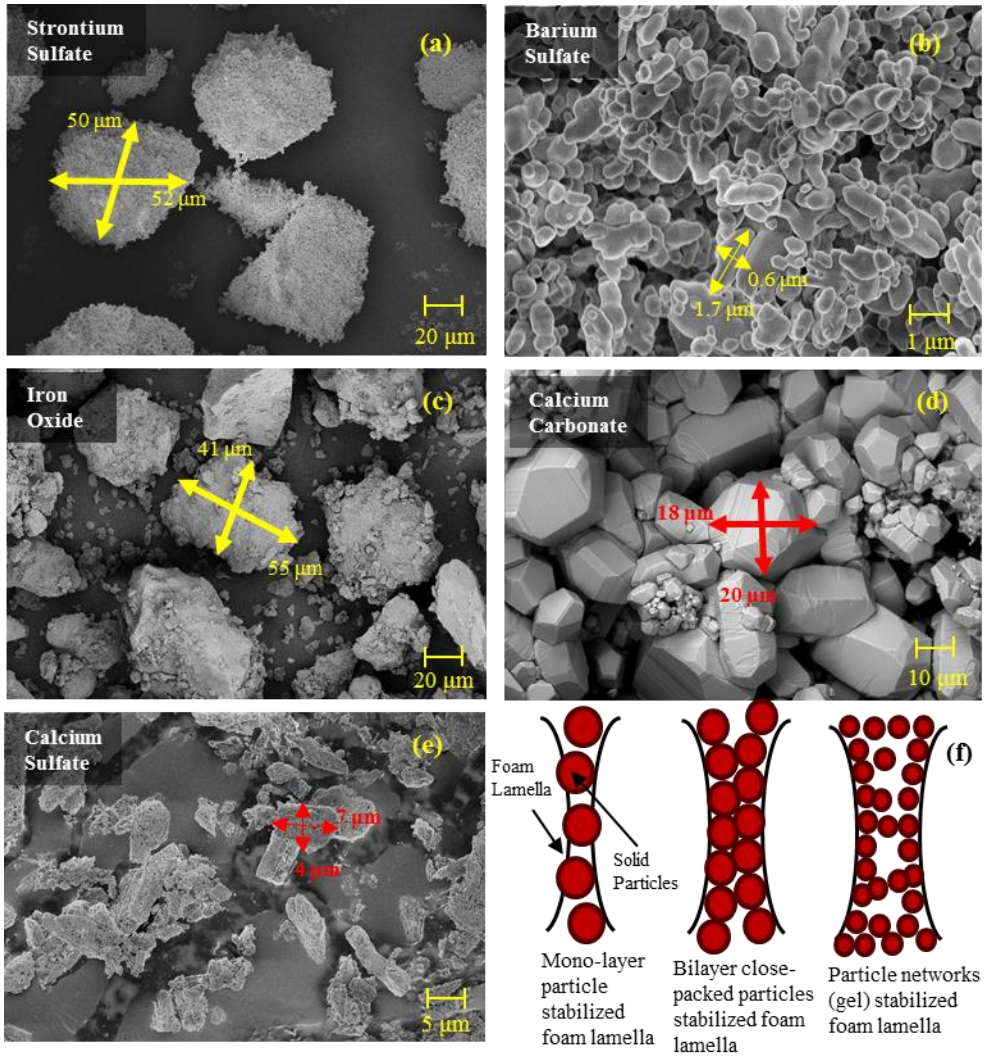

Figure13: Average particle size of different solid particles

Figure 13 shows SEM images of different particles used in this study. As can be seen in the Figure 13a and 13b, the average particle size for strontium sulfate is 50 times larger than barium sulfate which can probably make only monolayer particle stabilised foam lamellas.

It is also found that rounded solid particles stabilise bulk foam more than particles with sharp edges, since particles with sharp edges can easily break the lamellas by film bridging and dewetting mechanisms. Figure 14 presents the schematic effect of particle shape on bulk foam stability. As it is shown in this figure, foam breakage with round shaped particles occurs in four steps with different mechanisms. Initially, particles move into thick liquid film between gas bubbles and push the surfactant solution out of liquid film. This phenomenon

increases the interfacial tension in the area of liquid film as a result of decrease in surfactant concentration and liquid film thickness, which increases the disjoining pressure in foam lamella. In the next step rounded shape particle bridges foam lamella with a contact angle of more than 90° because of their geometry. The foam breakage usually happen faster and with particles with sharp edges solid particles as they skip lamella thinning (deweting) step and bridge the thick lamella foams directly.

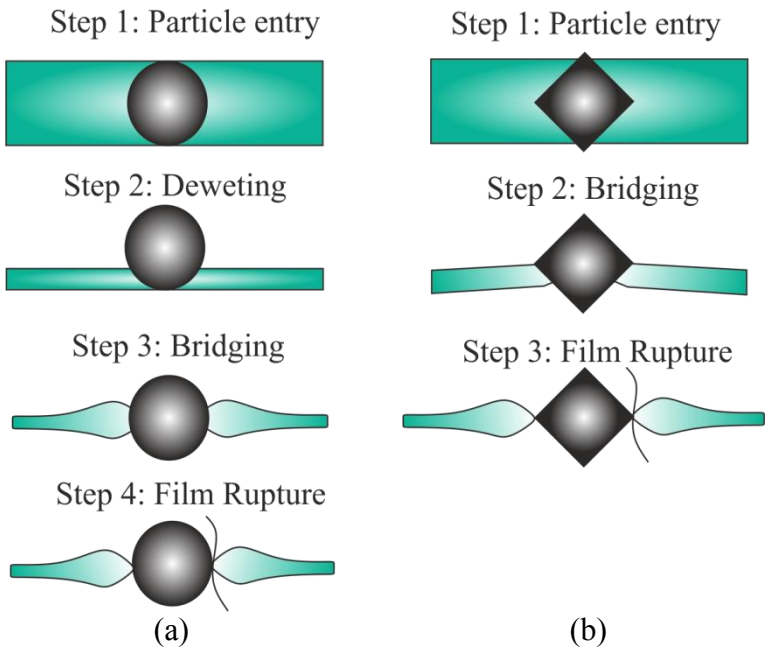

Figure14: Effect of particle shape on foam stability

Furthermore, in order to investigate the effect of solid particles on surface tension of AOS solution, a series of complementary experiments on surface tension were carried out using Du Noüy ring method. In these tests, surfactant concentration showed the dominant effect on surface tension reductions, and different solid particles used in this study, regardless of their concentration (0.05-0.5 wt%), have very negligible effect on surface tension of AOS solution. However, as calcium sulfate has higher adsorption rate of aqueous solution than the other solid particles discussed in this study, it contributes to a larger number of sulfate ions in bulk of aqueous phase, which in turn increase surface tension. Overall, as it is shown in Figure 15

other solid particles of calcium carbonate, barium sulfate, strontium sulfate and iron oxide do not have significant effect on surface tension of AOS solution.

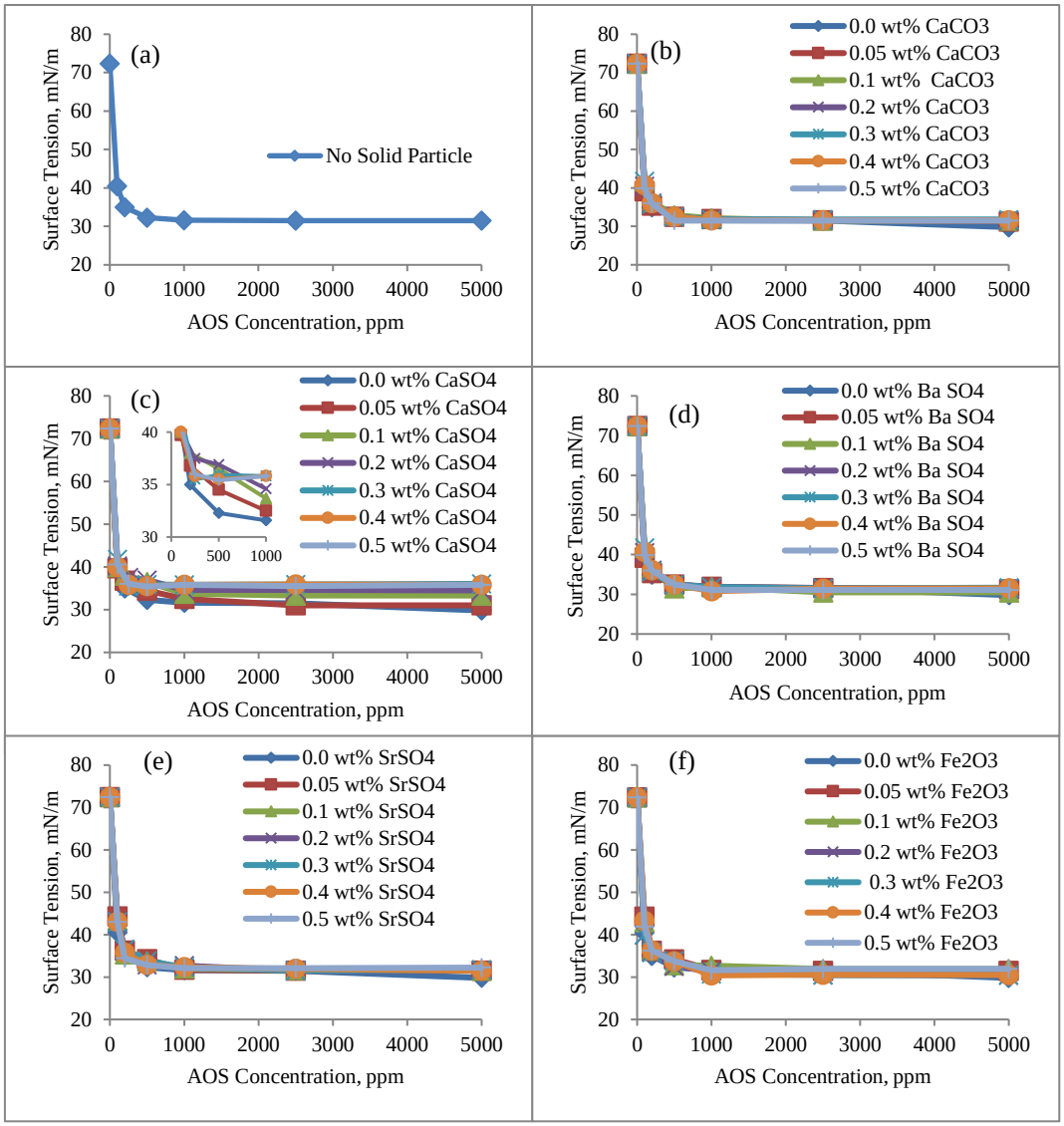

Figure 15: Surface tension of AOS solution in the absence and presence of solid particles (a) no solid particle, (b) calcium carbonate, (c) calcium sulfate, (d) barium sulfate, (e) strontium sulfate, (f) iron oxide (1 ppm of AOS solution = 3.17×10^{-6} mol/L)

Conclusions and Recommendations:

In this study we explored solid-fluids interactions between foam and solid particles. Stability, texture and rheological properties of foam in the presence of five solid particles of calcium carbonate, calcium sulfate, barium sulfate, strontium sulfate and iron oxide were tested. Each of these micro- and nano- particles shows its own characteristics of density, shape, size, and

ionic (wettability) properties in contact with foam generated by CO_2 and Sulfotex AOS surfactant. It was found that calcium carbonate, barium sulfate and strontium sulfate increase the stability of bulk foam through aggregation at the lamellae and plateau borders where they make liquid film of foam thicker, and as a result bubbles stay small and do not merge into each other easily. This enhanced stability is tempered by compound effects of density, shape, size and wettability, where round edges of small size and low density particles of calcium carbonate and barium sulfate are favourable. However, strontium sulfate showed less stable foam compared to barium sulfate and calcium carbonate as the particles are much larger and make monolayer bridges which induce disjoining pressure in the lamellas and destabilises foam by dewetting and film rupture.

Calcium sulfate and iron oxide on the other side destabilised bulk foam by liquid film rupture through different mechanisms. Calcium carbonate particles have predominantly hydrophilic property where they adsorb water inside the lamellae and plateau borders, leading to changes in contact angle and therefore a thinner liquid film and fast rupture.

These rheological properties and stabilising criteria can be investigated before running any foam-based enhanced oil recovery.

It is anticipated that hydrophobic particles absorb residual oil entrapped in porous media, however these particles may affect the persistence of foam and thus its performance. In this regard, the results of this study indicate that the hydrophobicity of particles may contribute to stability or instability of foams; thus their ability to recover oil from porous media should be considered for further investigation.

Acknowledgement:

The authors would like to acknowledge the school of engineering at the University of Aberdeen and University Technology Malaysia (UTM) to provide required materials and facilities to complete this research.

References:

[1] L. W. Lake, *Enhanced oil recovery*: Prentice Hall, 1989.

[2] E. C. Donaldson, G. V. Chilingarian, and T. F. Yen, *Enhanced Oil Recovery, II: Processes and Operations*: Elsevier Science, 1989.

[3] D. W. Green and G. P. Willhite, *Enhanced Oil Recovery*: Henry L. Doherty Memorial Fund of AIME, Society of Petroleum Engineers, 1998.

[4] Y. Ahmadi, S. E. Eshraghi, P. Bahrami, M. Hasanbeygi, Y. Kazemzadeh, and A. Vahedian, "Comprehensive Water–Alternating-Gas (WAG) injection study to evaluate the most effective method based on heavy oil recovery and asphaltene precipitation tests," *Journal of Petroleum Science and Engineering,* vol. 133, pp. 123-129, 9// 2015.

[5] M. Dong, J. Foraie, S. Huang, and I. Chatzis, "Analysis of Immiscible Water-Alternating-Gas (WAG) Injection Using Micromodel."

[6] S. M. Fatemi, M. Sohrabi, M. Jamiolahmady, S. Ireland, and G. Robertson, "Experimental Investigation of Near-Miscible Water-Alternating-Gas (WAG) Injection Performance in Water-wet and Mixed-wet Systems."

[7] L. Han and Y. Gu, "Optimization of Miscible CO2 Water-Alternating-Gas Injection in the Bakken Formation," *Energy & Fuels,* vol. 28, pp. 6811-6819, 2014/11/20 2014.

[8] M. Sohrabi, D. H. Tehrani, A. Danesh, and G. D. Henderson, "Visualization of Oil Recovery by Water-Alternating-Gas Injection Using High-Pressure Micromodels," 2004/9/1/.

[9] H. Belhaj, H. Abukhalifeh, and K. Javid, "Miscible oil recovery utilizing N2 and/or HC gases in CO2 injection," *Journal of Petroleum Science and Engineering,* vol. 111, pp. 144-152, 11// 2013.

[10] K. J. Hartman and A. S. Cullick, "Oil recovery by gas displacement at low interfacial tension," *Journal of Petroleum Science and Engineering,* vol. 10, pp. 197-210, 2// 1994.

[11] R. T. Johns and B. Dindoruk, "Chapter 1 - Gas Flooding A2 - Sheng, James J," in *Enhanced Oil Recovery Field Case Studies*, ed Boston: Gulf Professional Publishing, 2013, pp. 1-22.

[12] A. Satter and G. M. Iqbal, "17 - Enhanced oil recovery processes: thermal, chemical, and miscible floods," in *Reservoir Engineering*, ed Boston: Gulf Professional Publishing, 2016, pp. 313-337.

[13] M. R. Todd and G. V. Grand, "Enhanced oil recovery using carbon dioxide," *Energy Conversion and Management,* vol. 34, pp. 1157-1164, 9// 1993.

[14] A. Abedini and F. Torabi, "On the CO2 storage potential of cyclic CO2 injection process for enhanced oil recovery," *Fuel,* vol. 124, pp. 14-27, 5/15/ 2014.

[15] D. C. Boud and O. C. Holbrook, "Gas drive oil recovery process," ed: Google Patents, 1958.

[16] A. R. Kovscek and C. J. Radke, "Fundamentals of Foam Transport in Porous Media," in *Foams: Fundamentals and Applications in the Petroleum Industry*. vol. 242, ed: American Chemical Society, 1994, pp. 115-163.

[17] J. E. Hanssen and M. Dalland, "Gas-Blocking Foams," in *Foams: Fundamentals and Applications in the Petroleum Industry*. vol. 242, ed: American Chemical Society, 1994, pp. 319-353.

[18] R. Farajzadeh, A. Andrianov, and P. L. J. Zitha, "Investigation of Immiscible and Miscible Foam for Enhancing Oil Recovery," *Industrial & Engineering Chemistry Research,* vol. 49, pp. 1910-1919, 2010/02/17 2010.

[19] R. Rafati, H. Hamidi, A. K. Idris, and M. A. Manan, "Application of sustainable foaming agents to control the mobility of carbon dioxide in enhanced oil recovery," *Egyptian Journal of Petroleum,* vol. 21, pp. 155-163, 12// 2012.

[20] S. A. Farzaneh and M. Sohrabi, "Experimental investigation of CO2-foam stability improvement by alkaline in the presence of crude oil," *Chemical Engineering Research and Design,* vol. 94, pp. 375-389, 2// 2015.

[21] S. A. Jones, G. Laskaris, S. Vincent-Bonnieu, R. Farajzadeh, and W. R. Rossen, "Effect of surfactant concentration on foam: From coreflood experiments to implicit-texture foam-model parameters," *Journal of Industrial and Engineering Chemistry,* vol. 37, pp. 268-276, 5/25/ 2016.

[22] S. A. Jones, V. van der Bent, R. Farajzadeh, W. R. Rossen, and S. Vincent-Bonnieu, "Surfactant screening for foam EOR: Correlation between bulk and core-flood experiments," *Colloids and Surfaces A: Physicochemical and Engineering Aspects,* vol. 500, pp. 166-176, 7/5/ 2016.

[23] G. G. Bernard and L. W. Holm, "Effect of Foam on Permeability of Porous Media to Gas," 1964/9/1/.

[24] G. G. Bernard and W. L. Jacobs, "Effect of Foam on Trapped Gas Saturation and on Permeability of Porous Media to Water," 1965/12/1/.

[25] D. T. Wasan, K. Koczo, and A. D. Nikolov, "Mechanisms of Aqueous Foam Stability and Antifoaming Action with and without Oil," in *Foams: Fundamentals and Applications in the Petroleum Industry*. vol. 242, ed: American Chemical Society, 1994, pp. 47-114.

[26] L. L. Schramm and F. Wassmuth, "Foams: Basic Principles," in *Foams: Fundamentals and Applications in the Petroleum Industry*. vol. 242, ed: American Chemical Society, 1994, pp. 3-45.

[27] J. S. Lioumbas, E. Georgiou, M. Kostoglou, and T. D. Karapantsios, "Foam free drainage and bubbles size for surfactant concentrations below the CMC," *Colloids and Surfaces A: Physicochemical and Engineering Aspects,* vol. 487, pp. 92-103, 12/20/ 2015.

[28] Z. Li, Z. Liu, B. Li, S. Li, Q. Sun, and S. Wang, "Aqueous Foams Stabilized with Particles and Surfactants."

[29] M. Khajehpour, S. R. Etminan, J. Goldman, and F. Wassmuth, "Nanoparticles as Foam Stabilizer for Steam-Foam Process."

[30] Z. Du, M. P. Bilbao-Montoya, B. P. Binks, E. Dickinson, R. Ettelaie, and B. S. Murray, "Outstanding Stability of Particle-Stabilized Bubbles," *Langmuir,* vol. 19, pp. 3106-3108, 2003/04/01 2003.

[31] B. P. Binks and T. S. Horozov, "Aqueous Foams Stabilized Solely by Silica Nanoparticles," *Angewandte Chemie International Edition,* vol. 44, pp. 3722-3725, 2005.

[32] T. S. Horozov, "Foams and foam films stabilised by solid particles," *Current Opinion in Colloid & Interface Science,* vol. 13, pp. 134-140, 6// 2008.

[33] S. I. Karakashev, O. Ozdemir, M. A. Hampton, and A. V. Nguyen, "Formation and stability of foams stabilized by fine particles with similar size, contact angle and different shapes," *Colloids and Surfaces A: Physicochemical and Engineering Aspects,* vol. 382, pp. 132-138, 6/5/ 2011.

[34] Q. Sun, Z. Li, S. Li, L. Jiang, J. Wang, and P. Wang, "Utilization of Surfactant-Stabilized Foam for Enhanced Oil Recovery by Adding Nanoparticles," *Energy & Fuels,* vol. 28, pp. 2384-2394, 2014/04/17 2014.

[35] P. Nguyen, H. Fadaei, and D. Sinton, "Pore-Scale Assessment of Nanoparticle-Stabilized CO2 Foam for Enhanced Oil Recovery," *Energy & Fuels,* vol. 28, pp. 6221-6227, 2014/10/16 2014.

[36] B. Qin, Y. Jia, Y. Lu, Y. Li, D. Wang, and C. Chen, "Micro fly-ash particles stabilized Pickering foams and its combustion-retardant characteristics," *Fuel,* vol. 154, pp. 174-180, 8/15/ 2015.

[37] A. Carl, A. Bannuscher, and R. von Klitzing, "Particle Stabilized Aqueous Foams at Different Length Scales: Synergy between Silica Particles and Alkylamines," *Langmuir,* vol. 31, pp. 1615-1622, 2015/02/10 2015.

[38] A. A. Eftekhari, R. Krastev, and R. Farajzadeh, "Foam Stabilized by Fly Ash Nanoparticles for Enhancing Oil Recovery," *Industrial & Engineering Chemistry Research,* vol. 54, pp. 12482-12491, 2015/12/23 2015.

[39] S. Li, Z. Li, and P. Wang, "Experimental Study of the Stabilization of CO2 Foam by Sodium Dodecyl Sulfate and Hydrophobic Nanoparticles," *Industrial & Engineering Chemistry Research,* vol. 55, pp. 1243-1253, 2016/02/10 2016.

[40] Y. Zhang, Z. Chang, W. Luo, S. Gu, W. Li, and J. An, "Effect of starch particles on foam stability and dilational viscoelasticity of aqueous-foam," *Chinese Journal of Chemical Engineering,* vol. 23, pp. 276-280, 1// 2015.

[41] R. Singh and K. K. Mohanty, "Synergy between Nanoparticles and Surfactants in Stabilizing Foams for Oil Recovery," *Energy & Fuels,* vol. 29, pp. 467-479, 2015/02/19 2015.

[42] G. Zhao, C. Dai, D. Wen, and J. Fang, "Stability mechanism of a novel three-Phase foam by adding dispersed particle gel," *Colloids and Surfaces A: Physicochemical and Engineering Aspects,* vol. 497, pp. 214-224, 5/20/ 2016.

[43] M. D. Eisner, S. A. K. Jeelani, L. Bernhard, and E. J. Windhab, "Stability of foams containing proteins, fat particles and nonionic surfactants," *Chemical Engineering Science,* vol. 62, pp. 1974-1987, 4// 2007.

[44] A.-L. Fameau and A. Salonen, "Effect of particles and aggregated structures on the foam stability and aging," *Comptes Rendus Physique,* vol. 15, pp. 748-760, 10// 2014.

[45] P. R. Garrett, *The science of defoaming : theory, experiment and applications,* 2014.

[46] R. G. Alargova, D. S. Warhadpande, V. N. Paunov, and O. D. Velev, "Foam Superstabilization by Polymer Microrods," *Langmuir,* vol. 20, pp. 10371-10374, 2004/11/01 2004.

[47] Z. Xue, A. Worthen, A. Qajar, I. Robert, S. L. Bryant, C. Huh, *et al.*, "Viscosity and stability of ultra-high internal phase CO2-in-water foams stabilized with surfactants and nanoparticles with or without polyelectrolytes," *Journal of Colloid and Interface Science,* vol. 461, pp. 383-395, 1/1/ 2016.

[48] V. P. Kanawade, S. N. Tripathi, D. Bhattu, and P. M. Shamjad, "Sub-micron particle number size distributions characteristics at an urban location, Kanpur, in the Indo-Gangetic Plain," *Atmospheric Research,* vol. 147–148, pp. 121-132, //.

[49] U. T. Gonzenbach, A. R. Studart, E. Tervoort, and L. J. Gauckler, "Stabilization of Foams with Inorganic Colloidal Particles," *Langmuir,* vol. 22, pp. 10983-10988, 2006/12/01 2006.

[50] L. K. Petersen, C. K. Sackett, and B. Narasimhan, "High-throughput analysis of protein stability in polyanhydride nanoparticles," *Acta Biomaterialia,* vol. 6, pp. 3873-3881, 10// 2010.

[51] L. Klaus, Kazimierz, M., Dipl-Ing, W. G. and Dipl-Ing, B. M., "Method and procedure for swift characterization of foamability and foam stability," Europian Union Patent, 2004.

[52] J. Boos, W. Drenckhan, and C. Stubenrauch, "Protocol for Studying Aqueous Foams Stabilized by Surfactant Mixtures," *Journal of Surfactants and Detergents,* vol. 16, pp. 1-12, 2013.

[53] J. R. Calvert and K. Nezhati, "Bubble size effects in foams," *International Journal of Heat and Fluid Flow,* vol. 8, pp. 102-106, 1987/06/01 1987.

[54] G. J. Hirasaki and J. B. Lawson, "Mechanisms of Foam Flow in Porous Media: Apparent Viscosity in Smooth Capillaries," 1985/4/1/.

[55] K. Osei-Bonsu, N. Shokri, and P. Grassia, "Foam stability in the presence and absence of hydrocarbons: From bubble- to bulk-scale," *Colloids and Surfaces A: Physicochemical and Engineering Aspects*, vol. 481, pp. 514-526, 9/20/ 2015.